Analysis of Binding Interactions in an Idiotope−Antiidiotope Protein−Protein Complex by Double Mutant Cycles†

Ellen R. Goldman, William Dall'Acqua, Bradford C. Braden, and Roy A. Mariuzza*

Center for Advanced Research in Biotechnology, University of Maryland Biotechnology Institute, 9600 Gudelsky Drive, Rockville, Maryland 20850

Received July 18, 1996; Revised Manuscript Received September 24, 1996⊗

ABSTRACT: The idiotope−antiidiotope complex between the anti-hen egg white lysozyme antibody D1.3 and the anti-D1.3 antibody E5.2 provides a useful model for studying protein−protein interactions. A high-resolution crystal structure of the complex is available [Fields, B. A., Goldbaum, F. A., Ysern, X., Poljak, R. J., & Mariuzza, R. A. (1995) *Nature 374*, 739−742], and both components are easily produced and manipulated in *Escherichia coli*. We previously analyzed the relative contributions of individual residues of D1.3 to complex stabilization by site-directed mutagenesis [Dall'Acqua, W., Goldman, E. R., Eisenstein, E., & Mariuzza, R. A. (1996) *Biochemistry 35*, 9667−9676]. In the current work, we introduced single alanine substitutions in 9 out of 21 positions in the combining site of E5.2 involved in contacts with D1.3 and found that 8 of them play a significant role in ligand binding ($\Delta G_{mutant} - \Delta G_{wild\ type} > 1.5$ kcal/mol). Furthermore, energetically important E5.2 and D1.3 residues tend to be juxtaposed in the crystal structure of the complex. In order to further dissect the energetics of specific interactions in the D1.3−E5.2 interface, double mutant cycles were carried out to measure the coupling of 13 amino acid pairs, 9 of which are in direct contact in the crystal structure. The highest coupling energy (4.3 kcal/mol) was measured for a charged−neutral pair which forms a buried hydrogen bond, while side chains which interact through solvated hydrogen bonds have lower coupling energies (1.3−1.7 kcal/mol), irrespective of whether they involve charged−neutral or neutral−neutral pairs. Interaction energies of similar magnitude (1.3−1.6 kcal/mol) were measured for residues forming only van der Waals contacts. Cycles between distant residues not involved in direct contacts in the crystal structure also showed significant coupling (0.5−1.0 kcal/mol). These weak long-range interactions could be due to rearrangements in solvent or protein structure or to secondary interactions involving other residues.

The ability of proteins to form specific, stable complexes with other proteins is fundamental to many biological processes. Understanding the molecular basis of protein−protein recognition requires detailed characterization of individual interactions at the interface between the proteins. In general, the strength of an inter- or intramolecular interaction between two amino acid residues cannot be measured by simply mutating one of them because of the highly cooperative nature of protein structures. Interactions other than the interaction of interest are often disrupted, each of which contributes to the energetics of association (Ackers & Smiths, 1985; Serrano *et al*., 1990). These secondary effects include possible conformational changes in the proteins ranging from repositioning of side chains to movements in the backbone, as well as reorganizations in solvent structure in the vicinity of the mutation. Thus, comparing the binding of a wild-type protein with that of a mutant in which a side chain has been truncated gives an apparent binding energy which is generally greater than the incremental binding energy attributable to that side chain (Fersht, 1988). A more sophisticated approach to dissecting the energetics of pairwise interactions which overcomes most of the limitations of single mutant experiments makes use of so-called "double mutant cycles" (Carter *et al*., 1984; Ackers & Smith, 1985; Horovitz, 1987).

We have applied this method to study the energetics of binding of the anti-hen egg white lysozyme (HEL)[1] antibody D1.3 to the anti-D1.3 antibody E5.2. The crystal structure of this idiotope−antiidiotope complex is known to 1.9 Å resolution (Fields *et al*., 1995); furthermore, the Fv fragments (heterodimers consisting of only the light and heavy chain variable domains, V_L and V_H) of both D1.3 and E5.2 are readily produced in *Escherichia coli* and can be subjected to site-directed mutagenesis. Thus, this system constitutes an excellent model for providing detailed information on protein−protein interactions.

Specifically, FvD1.3(A) and FvE5.2(B) can be mutated (*i.e*., A → A′, B → B′) separately and together to construct the cycle:

$$\begin{array}{ccc} \text{FvD1.3(A)FvE5.2(B}') & \rightarrow & \text{FvD1.3(A}')\text{FvE5.2(B}') \\ \uparrow & & \uparrow \\ \text{FvD1.3(A)FvE5.2(B)} & \rightarrow & \text{FvD1.3(A}')\text{FvE5.2(B)} \end{array}$$

If the effects of the mutations are independent, the change in free energy for the double mutant is the sum of those for the two single mutations. But if there is an interaction between the mutated residues, the change in free energy for the double mutant is different from the sum of the two single

† This work was supported by NIH Grant GM52801 (R.A.M.).

* Author to whom correspondence should be addressed. Tel: 301-738-6243. Fax: 301-738-6255. E-mail: mariuzza@indigo2.carb.nist.gov.

⊗ Abstract published in *Advance ACS Abstracts,* December 15, 1996.

[1] Abbreviations: HEL, hen egg white lysozyme; scFv, single chain Fv fragment; RU, resonance units; CDR, complementarity-determining region; V_L, light chain variable region; V_H, heavy chain variable region.

S0006-2960(96)01769-2 CCC: $14.00

mutants (Ackers & Smith, 1985; Horovitz, 1987). In fact, this nonadditivity is the main obstacle to predicting the effect of a substitution on the association between two proteins. Assuming that the mutations do not introduce major structural changes in the complex, the differences in free energy on association can provide a quantitative estimate of the energy of interaction of the two side chains (A and B) based on the premise that the interactions of A and B with the rest of the interface will cancel out. The coupling, or interaction, energy between A and B ($\Delta\Delta G_{int}$) is given by

$$\Delta\Delta G_{int} = \Delta\Delta G_{AB\rightarrow AB'} - \Delta\Delta G_{A'B\rightarrow A'B'} = \Delta\Delta G_{AB\rightarrow A'B} - \Delta\Delta G_{AB'\rightarrow A'B'} \quad (1)$$

or when all the free energies are taken with reference to the wild-type complex:

$$\Delta\Delta G_{int} = \Delta\Delta G_{AB\rightarrow A'B} + \Delta\Delta G_{AB\rightarrow AB'} - \Delta\Delta G_{AB\rightarrow A'B'} \quad (2)$$

where each of the $\Delta\Delta G$ terms is determined by measuring the difference in the free energy of binding of the Fvs in the initial and final states of the corresponding transition.

To measure interaction energies, we systematically truncated the side chains of contact residues on both FvD1.3 and FvE5.2 by mutating them to alanine. We assumed that we did not introduce major changes in the framework of either antibody in the complex, as the mutations were introduced in the complementarity-determining regions (CDRs), whose conformations are less important for the conservation of the overall three-dimensional structure of the individual Fvs. To assure the accuracy of our results, affinities were measured using two independent techniques: surface plasmon resonance detection and analytical ultracentrifugation. We find that a large subset of contact residues on E5.2 contributes to the D1.3−E5.2 interaction, confirming previous results that the free energy of binding between two proteins may arise from many productive interactions distributed over the entire protein−protein interface (Dall'Acqua *et al*., 1996). Coupling energies were measured for 13 pairs of residues in the D1.3−E5.2 interface, 9 of which are in direct contact in the crystal structure. We show that these energies range from over 4 kcal/mol for the disruption of a buried hydrogen bond to approximately 1 kcal/mol for the disruption of van der Waals contacts. The importance of indirect coupling between residues is demonstrated by the determination of significant coupling energies for side chains which do not interact directly in the crystal structure. Thus, while the relative strengths of coupling energies in the FvD1.3−FvE5.2 interface were, in most cases, broadly consistent with expectations based on the three-dimensional structure, significant exceptions were also encountered, indicating that structural information alone is not always sufficient to predict binding energies in protein−protein complexes.

MATERIALS AND METHODS

Reagents. All chemicals were of analytical grade. Restriction enzymes and DNA-modifying enzymes were purchased from New England Biolabs, Inc. (Beverly, MA). Oligonucleotides were synthesized on a 308B DNA synthesizer (Applied Biosystems, Foster City, CA). Radiolabeled [^{35}S]dATP was obtained from Amersham Corp.

Protein Expression and Purification. The single chain versions of FvD1.3 (scFvD1.3; McCafferty *et al*., 1990) and of the mutants were expressed using the pUC19-based vector pSW1 (Ward *et al*., 1989) and isolated from the supernatants of recombinant *E. coli* BMH 71-18 cells (Dall'Acqua *et al*., 1996). The Fv fragments were purified by affinity chromatography using either monoclonal antibody E5.2− (Goldbaum *et al*., 1994) or HEL− (Boulot *et al*., 1990) Sepharose 4B columns. Production of FvE5.2 and its mutants was carried out as described (Dall'Acqua *et al*., 1996). A His_6 tail was grafted onto the 3′ of the V_L gene to permit purification using a nickel−nitrilotriacetic acid affinity column (QIAGEN).

Prior to BIAcore analysis, all Fv fragments were further purified by size exclusion chromatography on a ZORBAX GF-250 column (Dupont) in 0.2 M sodium phosphate, pH 7.4, in order to eliminate aggregated material which could interfere with affinity measurements (van der Merwe *et al*., 1994).

Site-Directed Mutagenesis. Site-directed mutagenesis of FvE5.2 and scFvD1.3 was performed using a Muta-Gene M13 in vitro mutagenesis kit (Bio-Rad, Richmond, CA) after subcloning the corresponding genes as *Eco*RI/Hi*nd*III fragments into M13mp18 (Kunkel *et al*., 1987). Mutagenic oligonucleotides were designed to replace the wild-type codon with the GCT codon for alanine. Mutations were confirmed by DNA sequencing (Sanger, 1977) using a Sequenase Version 2.0 kit (USB, Cleveland, OH).

Affinity Measurements. The interaction of soluble FvE5.2 with immobilized scFvD1.3 was measured by surface plasmon resonance detection using a BIAcore instrument (Pharmacia Biosensor, Uppsala, Sweden) essentially as described (Dall'Acqua *et al*., 1996), except that scFvD1.3 was coupled directly to the sensor chip, rather than first biotinylated to permit capture on a streptavidin-derivatized chip. Briefly, wild-type and mutant scFvD1.3 fragments were dialyzed against 10 mM sodium acetate, pH 5.0, and coupled to the dextran matrix of a CM5 sensor chip (Pharmacia Biosensor) using an amine coupling kit as described (Johnsson *et al*., 1991) at concentrations ranging from 25 to 100 μg/mL. Activation and immobilization periods were set between 3 and 7 min with a flow rate of 5 μL/min, and excess reactive esters were quenched by injecting 35 μL of 1.0 M ethanolamine hydrochloride, pH 8.5. Between 300 and 2000 resonance units (RU) of scFvD1.3 were typically immobilized under these conditions. Mutant FvE5.2 fragments were dialyzed against Hepes-buffered saline containing 150 mM NaCl, 0.005% Surfactant P-20 (Pharmacia), 3.4 mM EDTA, and 10 mM Hepes, pH 7.5. Dilutions of FvE5.2 ranging from 20 nM to 80 μM, depending on affinity, were made in the same buffer. Pulses of 10 mM HCl were used to regenerate the surfaces. To estimate the increase in RU resulting from the nonspecific effect of protein on the bulk refractive index, binding of FvE5.2 to a control surface with no immobilized ligand was also measured (data not shown). This nonspecific signal was generally not significant for analyte concentrations up to 1 μM. Following the last injection of FvE5.2, the analyte was reinjected at one of the initial concentrations to determine whether ScFvD1.3 had undergone significant denaturation as the result of repeated regenerations of the surface with 10 mM HCl. Very similar signals were obtained even following 15 regenerations,

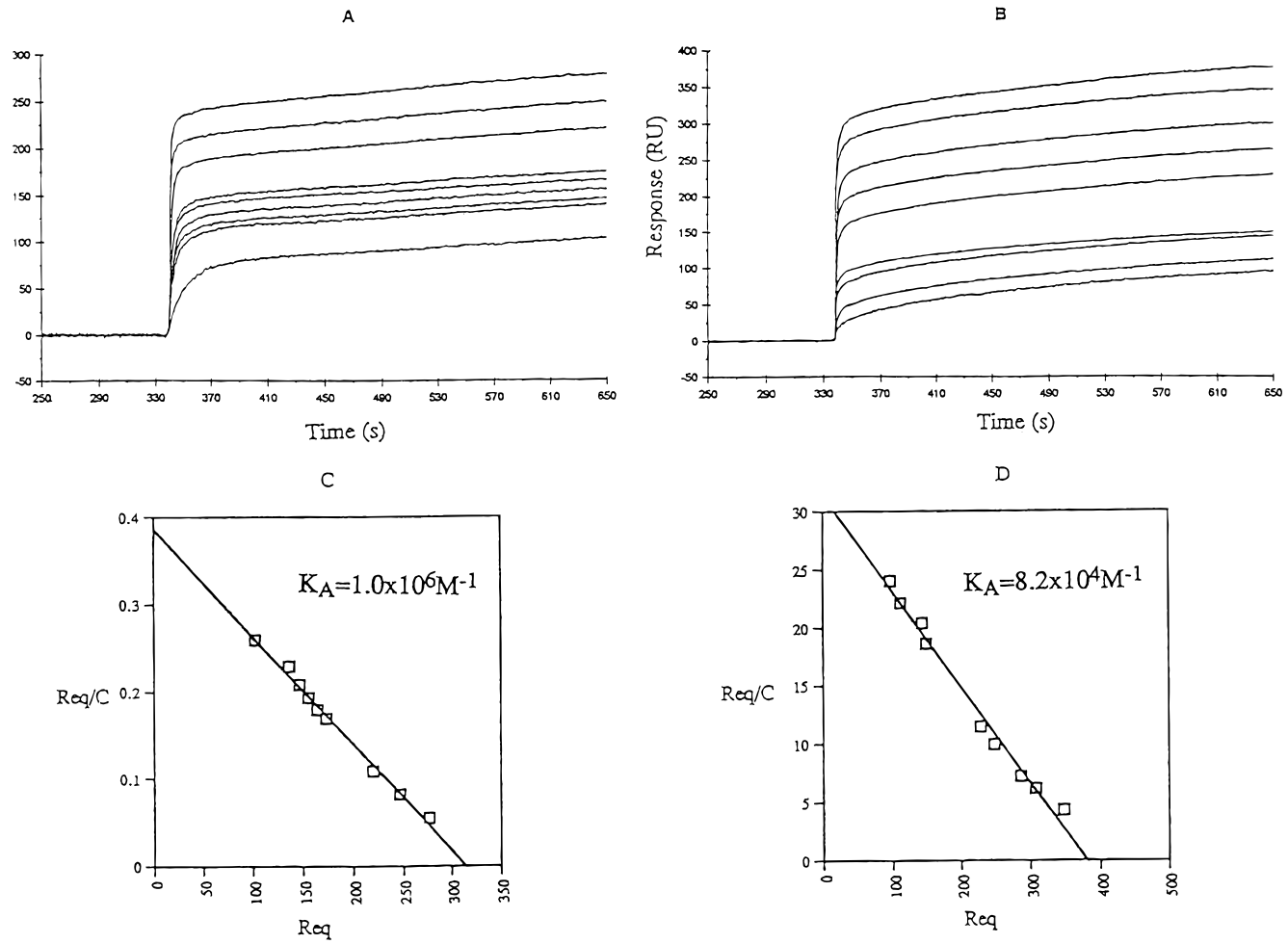

FIGURE 1: (A) Binding of FvE5.2V_HI97A to immobilized wild-type scFvD1.3. The E5.2 mutant was injected at concentrations ranging from 400 nM to 5 μM over a surface on which 480 RU of scFvD1.3 had been immobilized as described in Materials and Methods. (B) Binding of FvE5.2V_HQ100A to immobilized scFvD1.3V_HW52A. The E5.2 mutant was injected at concentrations ranging from 4 to 80 μM; 520 RU of the D1.3 mutant was immobilized on the chip. (C) Scatchard plot of the binding of FvE5.2V_HI97A to scFvD1.3 derived from the data in (A) after correction for nonspecific binding. The plot is linear with a correlation coefficient of 0.99. The apparent K_A is 1.0×10^6 M^{-1}. The predicted maximum binding capacity (315 RU) indicates that about 70% of the immobilized scFvD1.3 molecules are available for binding. (D) Scatchard plot derived from the data in (B) after correction for nonspecific binding. The plot is linear with a correlation coefficient of 0.99, and the apparent K_A is 8.2×10^4 M^{-1}. Over 70% of the immobilized scFvD1.3 is available for binding as calculated from the predicted maximum binding capacity (380 RU).

indicating that the immobilized ligand effectively retained its original binding activity.

The data were analyzed using the BIAevaluation 2.1 software package (Pharmacia). The concentration of complex can be assessed directly as the steady-state response when performing equilibrium binding experiments with BIAcore (Karlsson *et al*., 1991; van der Merwe *et al*., 1993, 1994; Malchiodi *et al*., 1995; Dall'Acqua *et al*., 1996), while the concentration of free analyte can be considered equal to the bulk analyte concentration since it is continuously replenished during sample injection. The concentration of free ligand on the surface of the sensor chip is then derived from the concentration of the complex and the total binding capacity of the surface. Association constants (K_As) were determined from Scatchard analysis, after correction for nonspecific binding, by measuring the concentration of free reactants and complex at equilibrium. Standard deviations for two or more independent K_A determinations were typically <30%.

Sedimentation equilibrium measurements were performed using a Beckman XL-A Optima analytical ultracentrifuge with a four-hole An-55 rotor. Experiments were carried out at 25 °C with a rotor speed of 25 000−28 000 rpm; samples were prepared in phosphate-buffered saline. Data were acquired as an average of 25 measurements of absorbance at each radial position with a nominal spacing of 0.001 cm between radial positions. For both scFvD1.3 and FvE5.2, a molar extinction coefficient of 36 000 M^{-1} cm^{-1} was used. Partial specific volumes were assumed to be 0.73 mL/mg, and solvent densities were determined pychnometrically. The data were analyzed as previously described (Malchiodi *et al*., 1995; Dall'Acqua *et al*., 1996) to yield association constants. Errors on K_As were about 20% of parameter values.

RESULTS AND DISCUSSION

Measurement of Association Constants for the Binding of FvE5.2 to scFvD1.3. Surface plasmon resonance profiles for equilibrium binding of the FvE5.2 mutant V_HI97A to immobilized wild-type scFvD1.3 and of FvE5.2V_HQ100A to scFvD1.3V_HW52A are shown in Figure 1 (panels A and B, respectively). To estimate apparent K_As, analyte concentrations ranging from 400 nM to 80 μM were used; higher concentrations were required to approach saturation for the

lower affinity E5.2V_HQ100A−D1.3V_HW52A interaction. The corresponding Scatchard plots, after correction for nonspecific binding, are shown in Figure 1 (panels C and D). The plots were linear, and apparent K_As were calculated as the slopes of the straight lines. The predicted maximum specific binding, calculated from the *x*-intercept assuming a linear relationship between the mass of bound protein and the measured RU (Granzow *et al*., 1992), indicated that approximately 70% of the immobilized scFvD1.3 molecules were available for binding in both cases. Similar results were obtained for the other mutants in this study.

Affinity constants for the interaction of wild-type FvE5.2 with mutants of scFvD1.3 have been determined previously (Dall'Acqua *et al*., 1996). In these experiments, BIAcore measurements were confirmed by fluorescence quenching and sedimentation equilibrium, methods which do not require immobilization of either of the interacting species. Thus, the K_As determined by fluorescence quenching for the binding of wild-type scFvD1.3 and of a mutant, D1.3V_H-D58A, to FvE5.2 (2.7×10^8 M^{-1} and 1.7×10^7 M^{-1}) were found to agree to within a factor of 3 with the BIAcore values (9.3×10^7 M^{-1} and 6.2×10^6 M^{-1}, respectively). Similarly, the K_A for the interaction of scFvD1.3V_HW52A with FvE5.2 measured by sedimentation equilibrium (9.1×10^4 M^{-1}) was close to that measured by BIAcore (8.6×10^4 M^{-1}). We therefore concluded that the BIAcore method is appropriate for affinity measurements in the scFvD1.3−FvE5.2 system over a K_A range of 10^4−10^8 M^{-1}.

In the current set of experiments, we carried out additional equilibrium sedimentation measurements to independently check our BIAcore results (Table 1). The K_A values for the interactions scFvD1.3−FvE5.2V_HQ100A, scFvD1.3V_HD54A−FvE5.2V_LY49A, scFvD1.3V_HN56A−FvE5.2V_HQ100A, and scFvD1.3V_HW52A−FvE5.2V_HQ100A obtained by sedimentation equilibrium (1.8×10^6 M^{-1}, 1.1×10^5 M^{-1}, 5.4×10^6 M^{-1}, and 4.0×10^4 M^{-1}, respectively) are in reasonable agreement with those from BIAcore (5.9×10^6 M^{-1}, 4.7×10^4 M^{-1}, 7.5×10^6 M^{-1}, and 8.2×10^4 M^{-1}, respectively). The observed differences could be due to subtle effects on scFvD1.3 conformation and/or accessibility as a result of the immobilization procedure. Errors in the analysis of the sedimentation measurements could also lead to significant differences in calculated association constants if, for example, an Fv mutant had a higher tendency to form aggregates over the course of the ultracentrifugation run.

Although the BIAcore and sedimentation equilibrium techniques gave association constants which differed by a factor of 2−3, it is important to emphasize that the BIAcore measurements were extremely reproducible. On repeat measurements of affinity, we found that the errors on K_A from BIAcore were consistently less than 30%. Using the worst case of 30% error on K_A translates into an error on $\Delta\Delta G$ of ±0.2 kcal/mol and a $\Delta\Delta G_{int}$ error of ±0.3 kcal/mol. Therefore, the BIAcore method may be used to compare the binding of a series of closely related mutant proteins with a relatively high degree of precision.

Mapping the Energetics of the FvE5.2−scFvD1.3 Interface. Residues in the interface between D1.3 and E5.2 were subjected to alanine-scanning mutagenesis (Wells, 1991) in order to determine their relative contribution to the free energy of association. Substitution of D1.3 residues in contact with E5.2 in the crystal structure had previously shown that, although a number of "hot spots" (ΔG_{mutant} − $\Delta G_{wild\ type}$ > 4.5 kcal/mol) are clearly present, most of the contact residues (11 of 15) contribute significantly to ligand binding ($\Delta\Delta G$ > 1.5 kcal/mol; Dall'Acqua *et al*., 1996). In the present work, we focused on a set of D1.3 residues with an apparent free energy contribution to binding of 1.2 kcal/mol or greater (Table 1, section A). We first determined which E5.2 residues they interacted with by examining the high-resolution crystal structure of the FvD1.3−FvE5.2 complex (Fields *et al*., 1995). We then individually mutated these 9 residues (out of 19 total non-glycine E5.2 residues in contact with D1.3) to alanine and measured the affinity of the mutants for wild-type D1.3 (Table 1, section B). The most destabilizing alanine substitutions are located at posi-

Table 1: Association Constants and Relative Free Energy Changes for Single and Double Mutant Complexes[a]

D1.3	E5.2	K_A (M^{-1})	
WT	WT	$9.3 \pm 3.3 \times 10^7$	
	Section A		
D1.3	E5.2	K_A (M^{-1})	$\Delta\Delta G$ (kcal/mol)
V_HE98A	WT	$7.9 \pm 2.4 \times 10^4$	4.2
V_HD54A	WT	$6.7 \pm 2.0 \times 10^4$	4.3
V_HD58A	WT	$6.2 \pm 1.9 \times 10^6$	1.6
V_LY49A	WT	$5.0 \pm 1.5 \times 10^6$	1.7
V_LY32A	WT	$3.0 \pm 0.9 \times 10^6$	2.0
V_HN56A	WT	$1.3 \pm 0.4 \times 10^7$	1.2
V_HW52A	WT	$8.6 \pm 0.5 \times 10^4$	4.2
V_HD100A	WT	$8.3 \pm 2.5 \times 10^5$	2.8
	Section B		
D1.3	E5.2	K_A (M^{-1})	$\Delta\Delta G$ (kcal/mol)
WT	V_HY98A	$3.1 \pm 0.9 \times 10^4$	4.7
WT	V_LY49A	$4.0 \pm 1.2 \times 10^6$	1.9
WT	V_HQ100A	$5.9 \pm 1.8 \times 10^6$ ($1.8 \pm 0.5 \times 10^6$)	1.6
WT	V_HN54A	$4.0 \pm 1.2 \times 10^6$	1.9
WT	V_HR100bA	$9.3 \pm 2.8 \times 10^4$	4.1
WT	V_HK30A	$1.7 \pm 0.5 \times 10^7$	1.0
WT	V_HH33A	$4.0 \pm 1.2 \times 10^6$	1.9
WT	V_HD52A	$5.4 \pm 1.6 \times 10^6$	1.7
WT	V_HI97A	$1.0 \pm 0.3 \times 10^6$	2.7
	Section C		
D1.3	E5.2	K_A (M^{-1})	$\Delta\Delta G$ (kcal/mol)
V_HE98A	V_HY98A	$3.7 \pm 1.1 \times 10^4$	4.6
V_HD54A	V_LY49A	$4.7 \pm 1.4 \times 10^4$ ($1.1 \pm 0.3 \times 10^5$)	4.5
V_HD58A	V_HQ100A	$7.8 \pm 2.3 \times 10^6$	1.5
V_LY49A	V_HN54A	$3.0 \pm 1.2 \times 10^6$	2.0
V_LY32A	V_HR100bA	$3.6 \pm 1.1 \times 10^4$	4.6
V_HN56A	V_HQ100A	$7.5 \pm 2.3 \times 10^6$ ($5.4 \pm 1.6 \times 10^6$)	1.5
V_HW52A	V_HQ100A	$8.2 \pm 2.5 \times 10^4$ ($4.0 \pm 1.2 \times 10^4$)	4.2
V_HD100A	V_HH33A	$8.4 \pm 2.5 \times 10^4$	4.1
V_HD100A	V_HD52A	$6.3 \pm 1.9 \times 10^4$	4.3
V_LY49A	V_HH33A	$1.1 \pm 0.3 \times 10^6$	2.6
V_HD100A	V_HN54A	$9.3 \pm 2.8 \times 10^4$	4.2
V_HN56A	V_HN54A	$1.9 \pm 0.6 \times 10^6$	2.3
V_HN56A	V_HH33A	$1.3 \pm 0.4 \times 10^6$	2.5

[a] Affinity measurements were carried out by BIAcore as described in Materials and Methods. The numbers in parentheses are K_A values determined by sedimentation equilibrium. Residue numbering is according to Kabat *et al*. (1991). The notation V_HR100bA indicates that the arginine residue at position V_H100b was mutated to alanine. WT refers to wild-type antibody. Differences in free energy changes are calculated as the difference between the ΔGs of the mutant and wild-type reactions ($\Delta\Delta G = \Delta G_{mutant} - \Delta G_{wild\ type}$). Sections A and B show affinities and $\Delta\Delta G$s for single mutants of D1.3 and E5.2, respectively. Section C shows values for the double mutants.

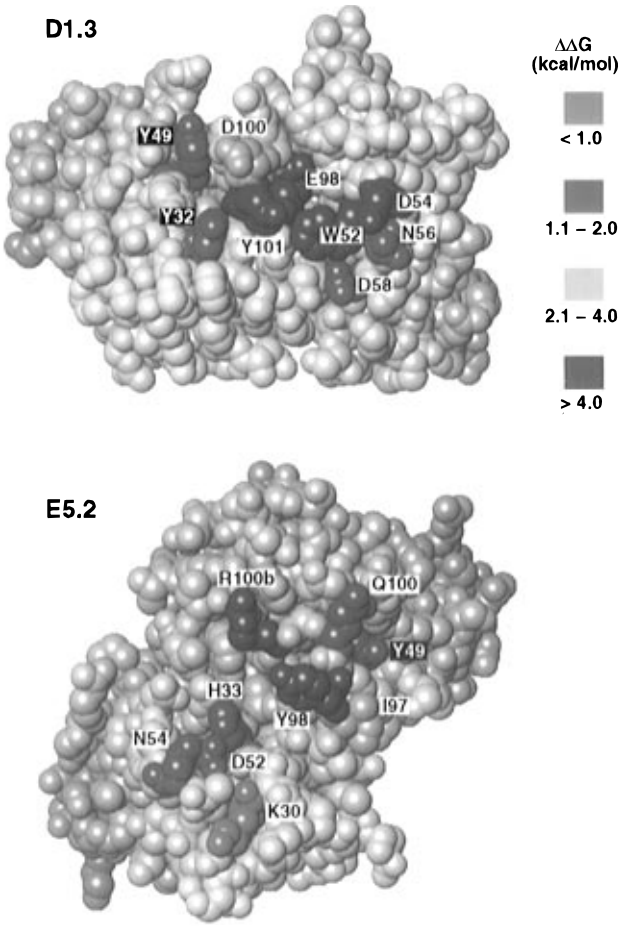

FIGURE 2: Space-filling models of the surface of FvD1.3 in contact with FvE5.2 and of the surface of FvE5.2 in contact with FvD1.3. The two Fv fragments are oriented such that they may be docked by folding the page along a horizontal axis between the components. Residues are color-coded according to the loss of binding free energy upon alanine substitution: red, >4.0 kcal/mol; yellow, 2.1−4.0 kcal/mol; green, 1.1−2.0 kcal/mol; blue, <1.0 kcal/mol. Labels with white backgrounds refer to V_H residues; labels with black backgrounds refer to V_L residues.

tions V_HY98 and V_HR100b ($\Delta\Delta G$ > 4.0 kcal/mol). Substitutions at the other seven positions tested (V_LY49, V_HK30, V_HH33, V_HD52, V_HN54, V_HI97, and V_HQ100) also resulted in significant effects on binding (1.0−2.8 kcal/mol). These results support the conclusion of Dall'Acqua *et al*. (1996) that stabilization of the D1.3−E5.2 complex is achieved by the accumulation of many productive interactions of varying strength over the entire interface between the two proteins. This is in contrast to the binding of D1.3 to HEL (Dall'Acqua *et al*., 1996) or of human growth hormone to its receptor (Cunningham & Wells, 1993; Clackson & Wells, 1995), where only a few interactions were found to dominate the energetics of the association reaction.

Figure 2 shows the residues of D1.3 and E5.2 important in complex stabilization mapped onto the three-dimensional structure of each Fv fragment. A comparison of the two functional epitopes reveals that hot spot positions on the E5.2 side of the interface generally correspond to hot spots on the D1.3 side. For example, E5.2 hot spot residues V_HY98 and V_HR100b make contact with D1.3 hot spot residues V_HE98 and V_HY101, respectively. Similarly, functionally less important residues of D1.3 and E5.2 tend to be juxtaposed in the interface between the two Fvs. For example, D1.3 residue V_LY49 ($\Delta\Delta G$ = 1.7 kcal/mol) interacts with the E5.2 residue V_HN54 (1.6 kcal/mol) in the crystal structure. This complementarity is in agreement with the observation of Clackson and Wells (1995) that energetically critical regions on human growth hormone match those on its corresponding receptor. These workers also noted that the functional epitopes pack together to form a hydrophobic core surrounded by hydrophilic residues, with substantial reductions in affinity occurring only on substitution of the hydrophobic ones. In contrast, our analysis of the D1.3−E5.2 system shows that both hydrophobic and hydrophilic, including charged, residues play a prominent role in complex stabilization and that there is not a clear segregation of hydrophilic residues at the periphery of the interface and of hydrophobic ones at the core (Figure 2). This may reflect the special character of antigen−antibody interactions in the sense that an antibody must recognize an antigenic surface regardless of the distribution of hydrophilic and hydrophobic residues. Further, the high frequency of tyrosines in antibody combining sites may be attributed to the amphipathic property of this residue, which permits tyrosines to engage in both hydrophobic and hydrogen-bonding interactions (Mian *et al*., 1991). Thus, one may define two broad categories of protein−protein interfaces: (i) ones which resemble cross sections through folded proteins in which hydrophobic residues are in the interior and hydrophilic ones at the periphery and in which productive binding is mediated largely by the former and (ii) ones in which polar and nonpolar residues are interspersed throughout the interface and in which both residue types make comparable contributions to complex stabilization.

Analysis of the Idiotope−Antiidiotope Interface Using Double Mutant Cycles. Double mutant cycles were constructed for 13 amino acid pairs in the FvD1.3−FvE5.2 interface in order to map the interaction energies at the contact surfaces between the two proteins (Table 1, section C). Of these 13 pairs, 9 had interacting side chains as judged from the crystal structure, whereas 4 were not expected to show coupling. We did not perform cycles in cases where a side chain of D1.3 or E5.2 contacts only the main chain of its partner (*e.g*., D1.3V_HR99 interacts with the main chain only of E5.2V_HK30 and E5.2V_HI97 contacts the main chain only of D1.3V_HT30).

Coupling energies were calculated according to eq 2. The interaction between D1.3V_HE98 and E5.2V_HY98 has the largest $\Delta\Delta G_{int}$, 4.3 kcal/mol (Table 2). These two residues form a buried hydrogen bond (D1.3V_HE98 $O^{\epsilon 1}\cdots O^{\eta}$ E5.2V_HY98) with good geometry in the crystal structure (Figure 3a). Our $\Delta\Delta G_{int}$ value for this residue pair is consistent with the energies measured for deletion of a hydrogen bond within a neutral−charged pair in other systems (about 4 kcal/mol; Fersht *et al*., 1985; Street *et al*., 1986; Fersht & Serrano, 1993). However, it is important to note that only part of the 4.3 kcal/mol is likely to be attributable to the hydrogen bond alone, since five van der Waals contacts should also be lost in the double mutant. In addition, a significant hydrophobic contribution can be expected from the burial of E5.2 residue V_HY98 upon complex formation. Thus, the measured coupling energy reflects the combination of a number of different atomic interactions. It is also worth noting that the values for hydrogen bond energies reported in the literature (Fersht *et al*., 1985; Street *et al*., 1986; Alber *et al*., 1987; Shirley *et al*., 1992; Serrano *et al*., 1992) were not obtained using double mutant cycles. Hence, they may

Table 2: Coupling Energies between the Indicated Amino Acid Pairs in the FvD1.3−FvE5.2 Complex As Measured by Double Mutant Cycles[a]

D1.3	E5.2	$\Delta\Delta G_{int}$ (kcal/mol)	type of interaction lost in double mutants (determined from crystal structure)
V_HE98	V_HY98	4.3	1 buried H bond and 5 van der Waals
V_HD54	V_LY49	1.7	1 solvated H bond and 3 van der Waals
V_HD58	V_HQ100	1.7	1 solvated H bond and 1 van der Waals
V_LY49	V_HN54	1.6	1 solvated H bond and 1 van der Waals
V_HW52	V_HQ100	1.6	3 van der Waals contacts
V_LY32	V_HR100b	1.5	2 van der Waals contacts
V_HN56	V_HQ100	1.3	3 van der Waals contacts
V_HD100	V_HH33	0.6	through zinc
V_HD100	V_HD52	0.2	through zinc
V_LY49	V_HH33	1.0	no direct contacts
V_HD100	V_HN54	0.5	no direct contacts
V_HN56	V_HN54	0.8	no direct contacts (far apart)
V_HN56	V_HH33	0.6	no direct contacts (far apart)

[a] Coupling energies are defined as $\Delta\Delta G_{int} = \Delta\Delta G_{AB\rightarrow A'B} + \Delta\Delta G_{AB\rightarrow AB'} - \Delta\Delta G_{AB\rightarrow A'B'}$, where $\Delta\Delta G_{AB\rightarrow A'B}$ is the change in binding free energy (relative to wild type) on mutation of D1.3 residue A to alanine (A′), $\Delta\Delta G_{AB\rightarrow AB'}$ is the change in binding energy on mutation of E5.2 residue B to alanine (B′), and $\Delta\Delta G_{AB\rightarrow A'B'}$ is the change in binding energy on mutation of both residues A and B to alanine. Intermolecular contacts were defined by atom pair distances (in Å) less than or equal to the following: C−C, 4.1: C−N, 3.8; C−O, 3.7, N−N, 3.4; N−O, 3.4; O−O, 3.3.

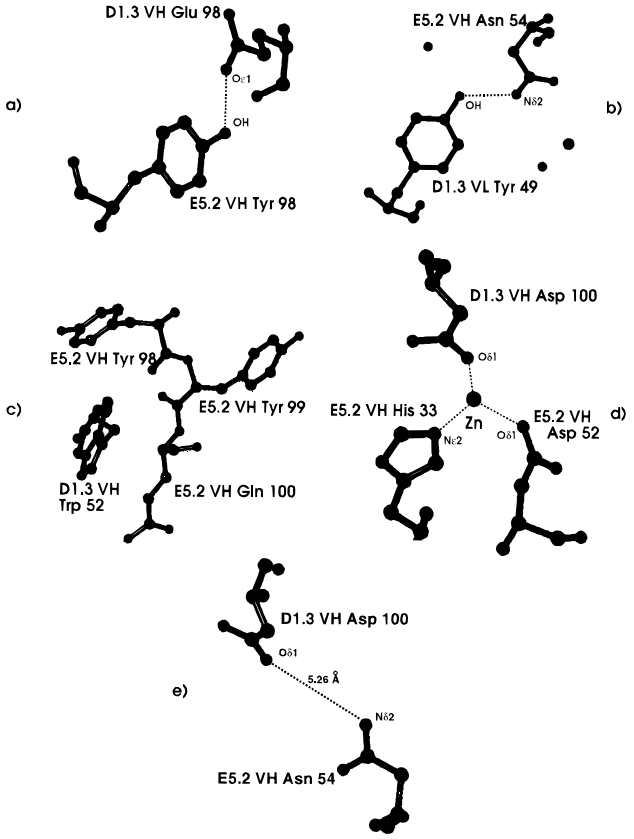

FIGURE 3: Illustrations of the types of interactions measured in the double mutant cycles. (a) Buried hydrogen bond between D1.3V_HE98 and E5.2V_HY98. (b) Solvent-exposed hydrogen bond between D1.3V_LY49 and E5.2V_HN54. (c) Van der Waals interactions between D1.3V_HW52 and E5.2V_HQ100. (d) Polar interactions of D1.3V_HD100 with E5.2 residues V_H33 and V_H52 mediated through a zinc atom in the crystal structure. (e) An example of two residues, D1.3V_HD100 and E5.2V_HN54, with no direct interactions.

significantly overestimate the intrinsic strength of these interactions.

Residues interacting through more solvent-exposed hydrogen bonds (D1.3V_HD54 $O^{\delta 2}\cdots O^{\eta}$ E5.2V_LY49, D1.3V_HD58 $O^{\delta 1}\cdots N^{\epsilon 2}$ E5.2V_HQ100, and D1.3V_LY49 $O^{\eta}\cdots N^{\delta 2}$ E5.2V_HN54) have significantly lower coupling energies (1.7, 1.7, and 1.6 kcal/mol, respectively; Table 2). In addition to the solvated hydrogen bonds, residues D1.3V_HD54 and E5.2V_LY49 (Figure 3b) make three van der Waals contacts, while the D1.3V_HD58−E5.2V_HQ100 and D1.3V_LY49−E5.2V_HN54 interactions include one additional van der Waals contact each. The $\Delta\Delta G_{int}$ values for these residue pairs are consistent with those found for deleting hydrogen bonds within neutral−neutral pairs (about 1.5 kcal/mol; Fersht *et al*., 1985; Street *et al*., 1986; Alber *et al*., 1987; Shirley *et al*., 1992; Serrano *et al*., 1992). However, the interactions between D1.3V_HD54 and E5.2V_LY49 and between D1.3V_HD58 and E5.2V_HQ100 involve charged−neutral pairs, for which coupling energies of about 4 kcal/mol might be expected. Since hydrogen bonds are essentially electrostatic interactions between atoms of opposite partial charge, this discrepancy may reflect, in part, a higher dielectric constant in the more peripheral regions of the FvD1.3−FvE5.2 interface which would tend to weaken the strength of such interactions. These results illustrate the importance of local environment, in addition to bond geometry and the magnitudes of the partial charges on the donor and acceptor atoms, in determining the relative strengths of different types of hydrogen bonds.

Residues which interact only through van der Waals contacts tend to show slightly lower coupling energies. The three pairs tested (D1.3V_HW52−E5.2V_HQ100, D1.3V_LY32−E5.2V_HR100b, and D1.3V_HN56−E5.2V_HQ100) make two or three van der Waals contacts between their side chains that are expected to be lost upon alanine substitution (Table 2). The highest coupling energy (1.6 kcal/mol) is observed between D1.3 residue V_HW52 and E5.2 residue V_HQ100. Alanine substitution should result in the loss of three side chain−side chain contacts, while a number of main chain−main chain interactions should be preserved (Figure 3c). A coupling energy of 1.3 kcal/mol was measured between D1.3V_HN56 and E5.2V_HQ100, in which three side chain−side chain van der Waals contacts should again be lost in the double mutant, and of 1.5 kcal/mol between D1.3V_LY32 and E5.2V_HR100b, in which only two such contacts should be lost. On this basis, we can calculate that each van der Waals contact contributes from 0.4 to 0.7 kcal/mol to complex stabilization. This is consistent with our previous estimate of 0.5 kcal/mol for contacts between carbon atoms derived from a calorimetric study of the binding of a mutant of FvD1.3, V_LW92D, to HEL (Ysern *et al*., 1994). However, these values should only be considered upper limits for the energies of van der Waals interactions in protein−protein interfaces since they almost certainly include significant contributions from the hydrophobic effect. These contributions may be particularly large for the D1.3V_HW52−E5.2V_HQ100 and D1.3V_LW92−HEL interactions as they involve tryptophan residues.

Two of the cycles, corresponding to residue pairs D1.3V_HD100−E5.2V_HH33 and D1.3V_HD100−E5.2V_HD52, yielded unexpectedly low coupling energies, 0.6 and 0.2 kcal/mol, respectively (Table 2); these values are as low as, or lower than, for certain quite distant residues (see below). In the crystal structure, these residues are linked through two polar interactions mediated by a Zn^{2+} ion from the crystallization

solution: D1.3V_HD100 $O^{\delta1}\cdots Zn^{2+}\cdots N^{\epsilon2}$ E5.2V_HH33 and D1.3V_HD100 $O^{\delta1}\cdots Zn^{2+}\cdots O^{\delta1}$ E5.2V_HD52 (Figure 3d). Although zinc was not present in the buffer used for affinity measurements (which also includes EDTA), residues D1.3V_HD100 and E5.2V_HH33 (but probably not D1.3V_HD100 and E5.2V_HD52, which are both negatively charged) might be expected to form direct or solvent-mediated hydrogen bonds in its absence. There are examples from studying the interaction of D1.3 with HEL in which hydrogen bonds mediated by peripheral water molecules are effectively neutral in energetic terms. The D1.3V_HD54A substitution decreases the K_A of the D1.3−E5.2 interaction by approximately 1000-fold but has little effect on the affinity of D1.3 for HEL (Dall'Acqua *et al*., 1996). This D1.3 residue makes direct hydrogen bonds to E5.2 but interacts with HEL through a bound water molecule. Likewise, the D1.3V_HE98A mutant has a much lower affinity for E5.2, with which it interacts through a direct hydrogen bond, than for HEL, where the hydrogen bond is solvent-mediated. In contrast, Perona *et al*. (1993) found that direct enzyme−substrate hydrogen bonds in the S1 site of trypsin do not significantly improve substrate binding relative to indirect water-mediated interactions.

Double mutant cycles were also constructed for four residue pairs not involved in direct interactions in the crystal structure: D1.3V_LY49−E5.2V_HH33, D1.3V_HD100−E5.2V_HN54 (Figure 3e), D1.3V_HN56−E5.2V_HN54, and D1.3V_HN56−E5.2V_HH33. The first two pairs are in proximity in the interface but do not form any direct contacts, while the second two are physically far apart (20−30 Å). The coupling energies for these interactions vary from 0.5 to 1.0 kcal/mol (Table 2). These values are significantly different from zero based on the experimental error of our measurements, ±0.3 kcal/mol (see above). Indeed, only one residue pair among the 13 examined (D1.3V_HD100−E5.2V_HD52; see above) has a coupling energy (0.2 kcal/mol) which is zero within experimental error. It is very likely, however, that a more extensive survey of noncontacting residues would reveal additional cases of zero (or negative) coupling. Small magnitude ($\leq$1 kcal/mol) energetic coupling between amino acid residues separated by large distances has been observed in several systems, including barnase−barstar (Schreiber & Fersht, 1995), staphylococcal nuclease (Green & Shortle, 1993), and human hemoglobin (Speros *et al*., 1991). These couplings tend to be unidirectional, either positive (as in the present case) or negative (LiCata & Ackers, 1995). The reason for this unidirectionality is unknown, but systematic errors in the data do not, for the most part, appear to be the explanation. As for the physical basis for the observed coupling between residues that are not in direct contact, there are several possible explanations (LiCata & Ackers, 1995). The assumption that the mutations do not have significant effects on protein conformation may not be valid. In addition, the mutations may introduce solvent rearrangements in the protein−protein interface, as described for a complex between a mutant of FvD1.3 and HEL (Ysern *et al*., 1994). Such changes, though localized, may result in long-range perturbations in electrostatic fields or vibrational modes within the interface.

Conclusions. We have shown that energetically important E5.2 and D1.3 residues are juxtaposed in the interface between the two proteins, with both hydrophobic and charged residues playing a prominent role in complex stabilization. The use of double mutant cycles has enabled us to quantitate the interaction between specific amino acid pairs in the complex. The highest coupling energy (4.3 kcal/mol) was measured for a charged−neutral pair forming a buried hydrogen bond. For residues interacting through solvent-exposed hydrogen bonds, coupling energies were approximately 1.7 kcal/mol, regardless of whether a neutral−neutral or charged−neutral pair was involved. Interactions formed by solvent-mediated hydrogen bonds were energetically neutral, at least in cases involving peripheral water molecules. Coupling energies of about 1.5 kcal/mol were measured for residues engaged only in van der Waals contacts. Ignoring the contribution of the hydrophobic effect to these interactions, we find that each van der Waals contact contributes approximately 0.5 kcal/mol to complex stabilization. However, dissociating the hydrophobic contribution to stabilization from that of other types of interactions will require characterizing a series of site-directed mutants in terms of both their thermodynamic properties (reaction enthalpies and entropies) and their three-dimensional structures (changes in buried surface area, packing density, and solvent structure). In this way, a comprehensive understanding of binding interactions in this protein−protein interface should emerge.

ACKNOWLEDGMENT

We are grateful to Michael Robinson (Pharmacia Biosensor), Emilio Malchiodi (CONICET, Argentina), and Edward Eisenstein for advice on affinity measurements. We thank Barry Fields for help in preparing the figures and for critical reading of the manuscript.

REFERENCES

Ackers, G. K., & Smith, F. R. (1985) *Annu. Rev. Biochem. 54*, 597−629.
Alber, T., Dao-Pin, S., Nye, J. A. Muchmore, D. C., & Matthews, B. W. (1987) *Biochemistry 26*, 3754−3758.
Carter, P. J., Winter, G., Wilkinson, A. J., & Fersht, A. R (1984) *Cell 38*, 835−840.
Chothia, C. (1974) *Nature 248*, 338−339.
Clackson, T., & Wells, J. A. (1995) *Science 267*, 383−386.
Cunningham, B. C., & Wells, J. A. (1993) *J. Mol. Biol. 234*, 554−563.
Dall'Acqua, W., Goldman, E. R., Eisenstein, E., & Mariuzza, R. A. (1996) *Biochemistry 35*, 9667−9676.
Eisenberg, D., & McLachlan, A. D. (1986) *Nature 319*, 199−203.
Fersht, A. R. (1988) *Biochemistry 27*, 1577−1580.
Fersht, A. R., & Serrano, L. (1993) *Curr. Opin. Struct. Biol. 3*, 75−83.
Fersht, A. R., Shi, J., Knill-Jones, J., Lowe, D. M., Wilkinson, A. J., Blow, D. M., Brick, P., Carter, P., Waye, M. M. Y., & Winter, G. (1985) *Nature 314*, 235−238.
Fields, B. A., Goldbaum, F. A., Ysern, X., Poljak, R. J., & Mariuzza, R. A. (1995) *Nature 374*, 739−742.
Goldbaum, F. A., Fields, B. A., Cauerhff, A., Ysern, X., Houdusse, A., Eisele, J. L., Poljak, R. J., & Mariuzza, R. A. (1994) *J. Mol. Biol. 241*, 739−743.
Granzow, R., & Reed, R. (1992) *Bio/Technology 10*, 390−393.
Hochuli, E., Bannwarth, W., Dobeli, H., Gentz, R., & Stuber, D. (1988) *Bio/Technology 6*, 1321−1325.
Horovitz, A. (1987) *J. Mol. Biol. 196*, 733−735.
Jin, L., Fendly, B. M., & Wells, J. A. (1992) *J. Mol. Biol. 226*, 851−865.
Johnsson, B., Lofas, S., & Lindquist, G. (1991) *Anal. Biochem. 198*, 268−277.
Kabat, E. A., Wu, T. T., Perry, H. M., Gottesman, K. S., & Foeller, C. (1991) *Sequences of Proteins of Immunological Interest*, U.S. Public Health Service, National Institutes of Health, Washington, DC.

Karlsson, R., Michaelsson, A., & Mattson, L. (1991) *J. Immunol. Methods 145*, 229−240.
Kunkel, T. A., Roberts, J. D., & Zakour, R. A. (1987) *Methods Enzymol. 154*, 367−382.
LiCata, V. J., & Ackers, G. K. (1995) *Biochemistry 34*, 3133−3139.
Malchiodi, E. L., Eisenstein, E., Fields, B. A., Ohlendorf, D. H., Schlievert, P. M., Karjalainen, K., & Mariuzza, R. A. (1995) *J. Exp. Med. 182*, 1833−1845.
McCafferty, J., Griffiths, A. D., Winter, G., & Chiswell, D. J. (1990) *Nature 348*, 552−554.
Mian, I. S., Bradwell, A. R., & Olson, A. J. (1991) *J. Mol. Biol. 217*, 133−151.
Nicholls, A., Sharp, K. A., & Honig, B. (1991) *Proteins*: *Struct., Funct., Genet. 11*, 281−296.
Novotny, J., Bruccoleri, R. E., & Saul, F. A. (1989) *Biochemistry 28*, 4735−4749.
Perona, J. J., Tsu, C. A., McGrath, M. E., Craik, C. S., & Fletterick, R. J. (1993) *J. Mol. Biol.* 934−949.
Sanger, F., Nicklen, S., & Coulson, A. R. (1977) *Proc. Natl. Acad. Sci. U.S.A. 74*, 5463−5467.
Schreiber, G., & Fersht, A. R. (1995) *J. Mol. Biol. 248*, 478−486.
Serrano, L., Horovitz, A., Avron, B., Bycroft, M., & Fersht, A. R. (1990) *Biochemistry 29*, 9343−9352.
Serrano, L., Kellis, J. T., Cann, P., Matouschek, A., & Fersht, A. R. (1992) *J. Mol. Biol. 224*, 783−804.
Shirley, B. A., Stanssens, P., Hahn, U., & Pace, C. N. (1992) *Biochemistry 31*, 725−732.
Speros, P. C., LiCata, V. J., Yontani, T., & Ackers, G. K. (1991) *Biochemistry 30*, 7254−7262.
Street, I. P., Armstrong, C. R., & Withers, S. G. (1986) *Biochemistry 25*, 6021−6027.
van der Merwe, P. A., Brown, M. H., Davis, S. J., & Barclay, A. N. (1993) *EMBO J. 12*, 4945−4954.
van der Merwe, P. A., Barclay, A. N., Mason, D. W., Davies, E. A., Morgan, B. P., Tone, M., Krishnam, A. K. C., Ianelli, C., & Davis, S. J. (1994) *Biochemistry 33*, 10149−10160.
Ward, E. S., Gussow, D., Griffiths, A. D., Jones, P. T., & Winter, G. (1989) *Nature 341*, 544−546.
Wells, J. A. (1991) *Methods Enzymol. 202*, 390−411.
Ysern, X., Fields, B. A., Bhat, T. N., Goldbaum, F. A., Dall'Acqua, W., Schwartz, F. P., Poljak, R. J., & Mariuzza, R. A. (1994) *J. Mol. Biol. 238*, 496−500.

BI961769K